



Energy consumption analysis of a supercritical water oxidation pilot plant with a transpiring wall reactor based on energy recovery

Fengming Zhang^{a,b}, Shouyan Chen^a, Chunyan Xu^a, Guifang Chen^a, Chunyuan Ma^{a,*}

^aNational Engineering Laboratory for Coal-fired Pollutants Emission Reduction, Shandong University, No. 17923, Jingshi Road, Jinan 250061, Shandong Province, China

Tel. +86 0531 88399369; Fax: +86 0531 88395877; email: sdetechym@163.com

^bGuangzhou Institutes of Advanced Technology, Chinese Academy of Sciences, No. 1121, Haibin Road, Nansha District, Guangzhou 511458, Guangdong Province, China

Received 29 February 2012; Accepted 24 February 2013

ABSTRACT

Supercritical water oxidation (SCWO) is a new and promising technology for treating organic waste and recovering energy. High energy consumption is a major problem preventing its commercial application. Energy recovery is the most effective method for reducing energy consumption of an SCWO system. To maximize the energy recovery of the SCWO pilot plant with a transpiring wall reactor, the reactor effluent is used to preheat both feed and transpiring water and produce hot water. An experimental study was conducted to investigate the influence of the operating parameters on energy consumption per unit total organic carbon (TOC) removal (ECPT) for saving the energy of the system. Results show that the effect of feed concentration on ECPT is the most significant and that of high feed concentrations, result in lower ECPT. Lower ECPT is also present at high feed flow rates, but at the expense of the decrease of TOC removal efficiency when the feed flow rate exceeds 14 kg/h.

Keywords: Supercritical water oxidation; Transpiring wall reactor; Energy recovery; Hot water; Energy consumption per unit TOC removal

1. Introduction

Supercritical water oxidation (SCWO) is a new and promising technology for treating organic waste and recovering energy [1]. It usually operates above the critical point of water ($P_C = 22.1$ MPa, $T_C = 374.3^\circ\text{C}$), using oxygen or other oxidants to make organic compounds combust. The thermo-physical properties of supercritical water are quite different from those at ambient conditions, and its solvent and reaction char-

acteristics drastically change [2]. Supercritical water is a good solvent for nonpolar organic compounds and gases such as oxygen, nitrogen, or carbon dioxide [3]. In a single-phase mixture of organic compounds and oxygen in supercritical water, mass transfer resistances are absent [4]. A residence time of only a few seconds or one minute is required to destroy the organic compounds and ensure a fast reaction rate [5,6]. The oxidation reaction does not result in any SO_2 and NO_x byproduct because of its lower reaction temperature compared with incineration [7].

*Corresponding author.

The superiority of SCWO is undeniable, and some devices have been designed for industrial applications [8–10]. However, some technical problems still exist, such as corrosion, salt plugging, and high investment cost, which constrain its commercialization [11,12]. The transpiring wall reactor is a promising solution to solve the problems of corrosion and salt plugging by fluid dynamic means [9,13,14]. This reactor concept includes a dual shell consisting of an outer pressure-resistant vessel and an inner porous vessel. Transpiring water at subcritical temperature passes through the porous pipe to form a film or at least a driving force directed to the center of the inner reactor. The transpiring effect can avoid solids or precipitated salts from sticking to the inner surface of the porous tube, thereby improving corrosion resistance [9].

Pressurization and heating are the essential steps in the SCWO process, and energy requirement is considerably high [15]. Energy recovery from the effluent is the leading method for reducing energy consumption, hence reducing operational cost.

Autothermal operation is a great concern in the SCWO process. The minimal heating value of feed stream required for SCWO without any electric heating was determined by theoretical calculation [15] or process simulation [16,17]. Power generation is another solution for energy recovery. The direct power generation of stream from the reactor has been visualized by Bermejo et al. [18]. The presence of particles will lead to the significant reduction of a stream turbine's lifetime. However, the idea of Bermejo may depend on a gas–solid separator at 650°C and 25 MPa which does not exist nowadays for technical reasons. Better solutions for power generating would be the use of an auxiliary fluid [16,19,20]. Although, work may determine energy self-sufficiency in theory, they also concluded that the power generation efficiency is usually too low. Furthermore, we should note that the addition of a set of power plant equipments will greatly increase the investment cost; therefore, power generation for energy recovery appears less realistic.

In a transpiring wall SCWO system, large amounts of transpiring water at a certain temperature (usually below 374°C) will be injected into the reactor to protect the transpiring wall [21,22]. Additional energy will, thus, be consumed compared with the traditional SCWO system. However, the outflow temperature of a transpiring wall reactor is usually below the critical value of water [23,24]. Given that the appropriate temperature of a reactor effluent for autothermal or electricity generation is 450 to –650°C, other solutions for maximum energy recovery such as producing hot water [8,25,26], can be considered as an alternative in the transpiring wall SCWO system.

In the present paper, experiments were conducted on a transpiring wall SCWO pilot plant equipped with an energy recovery system using methanol solution as artificial wastewater. We provide an alternative to maximize the energy recovery in transpiring wall SCWO pilot plant; the reactor effluent was used to preheat both feed and transpiring water, and produce hot water. The energy consumption of the new process is estimated by energy consumption per unit TOC removal (ECPT). The influence of the operating parameters (feed concentration, feed temperature, feed flow rate, transpiration intensity, and the temperature of the upper branch of transpiring water) on TOC removal efficiency and ECPT was investigated to find out the appropriate operating parameters for the pilot plant.

2. Experiment

2.1. Experimental setup

The diagram of the SCWO pilot plant with a transpiring wall reactor in Shandong University is presented in Fig. 1. Five streams are introduced into the reactor. The feed stream is pressurized by an air driven liquid pump (Haskel, model DSTV-60), that supplies flow at 0.5–25 kg/h. The oxygen stream is pressurized by an air driven gas pump (Haskel, model AGT-15/75) that supplies flow at 0.05–4 kg/h. The transpiring water (tw) stream is pressurized by an air driven liquid pump (Haskel, model ASF-60) that supplies flow at 0–100 kg/h, which is then divided into three branches by three mass flow control valves (SLPMMV26 V): the upper branch of transpiring water (tw1), the middle branch of transpiring water (tw2), and the lower branch of transpiring water (tw3). The liquid pumps and the gas pump are driven by a screw air compressor with a flow rate of 2 m³/min and an outlet pressure of 0.8 MPa. The flow rates of all the streams are adjusted manually by flow control valves (SLPMMV26 V) and are measured by Coriolis-type mass flow meters (accuracy: ±1%). The pressure of all the streams is adjusted by pressure reducing valves (TESCOM, 44–1100 Series) and measured by pressure gauges and pressure transducers (0–40 MPa, accuracy: ±0.5%). Feed, the upper branch of transpiring water, and the middle branch of transpiring water are heated to desired temperatures by electric heater 1(e1), electric heater 2(e2), and electric heater 3(e3), respectively. Oxygen and the lower branch of transpiring water (tw3) pass through the reactor without being preheated.

The outer vessel of the transpiring wall reactor is made of stainless steel 321, with inner and outer

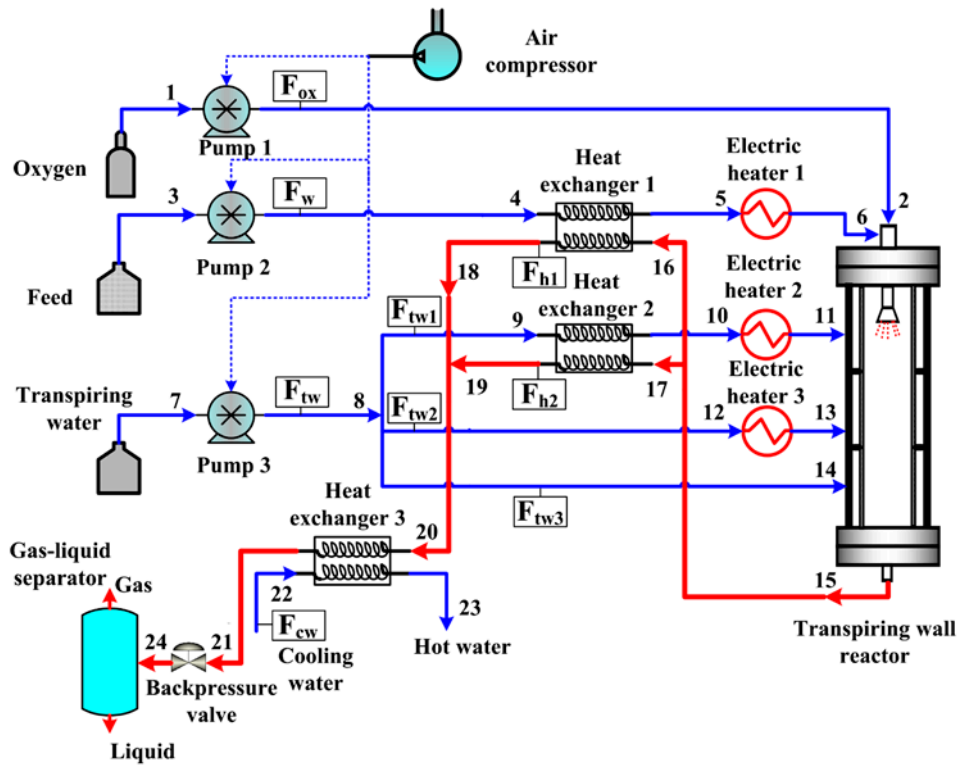


Fig. 1. The diagram of the SCWO pilot plant with a transpiring wall reactor in Shandong University (“numerics” indicate stream numbers).

diameters of 80 and 114 mm, respectively. The inner porous tube is made of porous sintered stainless steel 316L, with inner and outer diameters of 55 and 60 mm, respectively. The transpiring wall reactor has

an effective reaction volume of about 1.8L. Pore size and porosity of the porous tube are 20.8 μm and 42.7%, respectively. The transpiring wall is divided into three zones using two retaining rings. More details of the reactor are shown in Fig. 2.

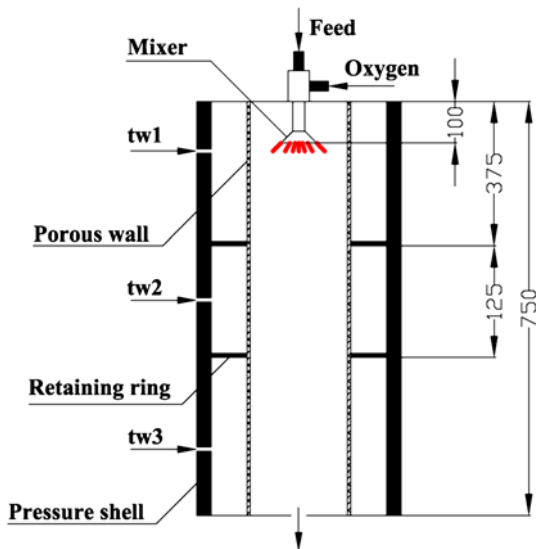


Fig. 2. The scheme of the transpiring wall reactor.

Three tubular countercurrent heat exchangers are arranged at the pilot plant to reduce energy consumption. The reactor effluent is initially split into two streams by two mass flow control valves (10VRMM2812): one is used to preheat feed stream in heat exchanger 1 (h1) and the other is used to preheat transpiring water in heat exchanger 2 (h2). The remaining energy can be recovered by heat exchanger 3 (h3) to supply hot water externally. The three heat exchangers have same configuration, but the lengths are different: 30 m for h1 and h2 and 20 m for h3. The central tube of the heat exchanger has internal and external diameters of 5 and 10 mm, respectively. The outer tube has internal and external diameters of 13 and 19 mm, respectively.

The pressure of the effluent after being cooled by heat exchangers will be reduced to ambient pressure by a back pressure valve (TESCOM, 26–1700 Series, accuracy: ±1%). Finally, the water–gas mixture will be introduced into a gas–liquid separator, and samples

will be collected and analyzed. The devices and the pipes of the pilot plant are covered with thermal insulation layer to minimize the heat loss. Process data are monitored and recorded using data acquisition software in a computer. Further details about the pilot plant can be found elsewhere [27].

2.2. Material and analytical method

Oxygen (purity >99.9%) was used as oxidant in the experiment. Desalinated water was used as transpiring water, with its electric conductivity less than 10 μs . Desalinated water-methanol (purity >99.9%) mixture was used as artificial wastewater which is called “feed” in this paper. The liquid samples were collected every 10 min for analysis, when the system pressure, the mass flow, and temperature of all steams and the reaction temperature inside the reactor were stable, and then it would be analyzed by a TOC 5000A shimadzu total organics carbon analyzer. The temperatures of each stream were measured by PT100 resistance thermometers (-200 to 500°C , accuracy: $\pm 0.5\%$). Energy consumption of air compressor and electric heaters was recorded by power meters.

3. Parameters definition

3.1. Transpiration intensity

The mass flow of transpiring water was fixed using a transpiration intensity R defined as follows [28]:

$$R = \frac{(F_{tw1} + F_{tw2} + F_{tw3}) / (A_{tw1} + A_{tw2} + A_{tw3})}{(F_w + F_{ox}) / A_b} \quad (1)$$

where F_{tw1} , F_{tw2} , and F_{tw3} are the mass flow of $tw1$, $tw2$, and $tw3$, respectively; F_{ox} and F_w are the mass flow rate of oxygen and feed, respectively; A_b is the inner circular area. A_{tw1} , A_{tw2} , and A_{tw3} are the inner shell surfaces of the three transpiring zones, respectively. The same transpiring intensities of the three transpiring zones are set in the experiments.

3.2. TOC removal efficiency

TOC removal efficiency (X) is defined as the mass of total organic carbon eliminated by the total organic carbon introduced into the reactor in Eq. (2). TOC_{in} and TOC_{out} symbolize the inlet and outlet concentration of TOC at stable condition, respectively [29].

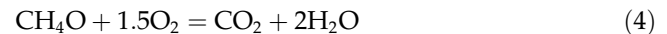
$$X = \frac{F_w \text{TOC}_{in} - (F_w + F_{tw1} + F_{tw2} + F_{tw3}) \text{TOC}_{out}}{F_w \text{TOC}_{in}} \quad (2)$$

3.3. Energy consumption

ECPT can be defined in Eq. (3).

$$\text{ECPT} = \frac{Q_c + Q_{e1} + Q_{e2} + Q_{e3} - Q_{h3}}{F_w \text{TOC}_{in}} \quad (3)$$

Q_c is the energy consumed by air compressor. Q_{e1} , Q_{e2} , and Q_{e3} are the energy consumed by $e1$, $e2$, and $e3$, respectively. Q_{h3} is the energy recovered by $h3$. From the definition of ECPT, it is a parameter which is based on the energy consumption of the system and TOC removal efficiency. In the transpiring wall SCWO system, the energy input includes electric energy consumed by air compressor (Q_c) and three electric heaters (Q_{e1} , Q_{e2} , and Q_{e3}). The reaction heat of methanol (Q_r) based on complete oxidation can be calculated by Hess' law shown as follows:



$$q_r = \frac{1}{M} ((\Delta H_f^0)_{\text{CO}_2} + 2(\Delta H_f^0)_{\text{H}_2\text{O}} - (\Delta H_f^0)_{\text{CH}_4\text{O}} - 3/2(\Delta H_f^0)_{\text{O}_2}) \quad (5)$$

$$Q_r = F_w \omega q_r X \quad (6)$$

Taking into consideration that SCWO is a wastewater treatment technology, Q_r is costless, and therefore should be excluded from the energy consumption of the system.

There are three heat exchangers for recovering energy in the pilot plant. Energy recovered by $h1$ (Q_{h1}) and $h2$ (Q_{h2}) are used for internal consumption to preheat feed and transpiring water, thus reducing energy consumption of $e1$ and $e2$. The energy recovered by $h3$ (Q_{h3}) will be used to supply hot water externally, which can partially offset the energy consumption of the system. Energy recovery by heat exchanger is calculated by the enthalpy gain of cold stream, which is dependent on pressure (can be considered as constant), temperature, and composition of stream. The energy recovered by heat exchangers can be calculated as follows:

$$Q_{h1} = F_w (h_5 - h_4) \quad (7)$$

Table 1
The operating condition and results discussed in this work

No.	$F_w / \text{kg h}^{-1}$	R	$F_{tw1} / \text{kg h}^{-1}$	$F_{tw2} / \text{kg h}^{-1}$	$F_{tw3} / \text{kg h}^{-1}$	γ^a	$\omega / \text{wt.}\%$	$F_{h1} / \text{kg h}^{-1}$	$F_{h2}^b / \text{kg h}^{-1}$	$t_5 / ^\circ\text{C}$	$t_6 / ^\circ\text{C}$	$t_{10} / ^\circ\text{C}$	$t_{11} / ^\circ\text{C}$	$t_{13} / ^\circ\text{C}$	$t_{15}^c / ^\circ\text{C}$	$t_{18} / ^\circ\text{C}$	$t_{19} / ^\circ\text{C}$	$t_{20} / ^\circ\text{C}$	$t_{21}^d / ^\circ\text{C}$	$t_{23}^e / ^\circ\text{C}$	URT ^f / s
A1	9.9	0.060	17.27	5.76	11.52	2.21	2	28.5	21.1	271	418	272	358	272	292	135	93	110	30	61	13.7
A2	10.1	0.061	18.74	6.25	12.49	1.92	4	32.3	23.0	282	420	283	357	280	303	139	100	115	30	64	14.1
A3	9.9	0.058	18.68	6.23	12.45	2.14	6	26.3	18.7	294	421	299	361	273	308	148	109	122	29	65	16.2
A4	9.9	0.058	19.98	6.66	13.32	2.30	8	27.3	19.5	305	417	306	358	269	325	151	114	127	30	68	18.4
B1	10.0	0.061	19.33	6.44	12.89	1.80	6	32.0	23.8	292	369	293	363	269	286	143	85	113	22	65	17.4
B2	9.9	0.060	19.28	6.43	12.85	2.11	6	27.9	21.0	297	390	298	363	271	294	154	91	120	23	66	14.6
B3	9.9	0.062	19.65	6.55	13.10	1.93	6	32.3	23.9	299	410	301	363	268	297	159	93	123	24	68	14.2
B4	9.9	0.059	18.83	6.28	12.55	2.02	6	27.1	20.1	300	419	302	362	272	299	161	96	133	26	69	14.6
C1	8	0.039	10.03	3.34	6.68	1.98	6	18.3	13.6	228	418	223	343	225	247	73	60	68	30	36	17.2
C2	11	0.039	13.77	4.59	9.18	1.97	6	24.7	18.3	273	423	266	343	226	287	91	79	86	26	51	12.5
C3	14	0.039	17.64	5.88	11.76	2.05	6	29.9	22.2	302	421	293	343	223	312	115	103	110	27	58	11.5
C4	17	0.040	21.95	7.32	14.63	2.04	6	37.4	26.8	312	419	303	341	225	319	129	115	123	27	75	10.0
D1	8.8	0.04	11.36	3.79	7.58	2.04	6	19.4	14.4	275	414	269	336	234	291	102	83	94	24	46	18.7
D2	8.9	0.05	14.39	4.80	9.59	2.06	6	22.8	16.9	267	414	261	336	231	282	116	78	100	24	52	16.3
D3	8.9	0.06	17.28	5.76	11.52	2.07	6	25.4	18.8	263	415	258	337	231	276	124	74	103	24	57	16.1
D4	8.9	0.07	20.13	6.71	13.42	2.05	6	29.4	21.8	258	415	254	335	231	269	137	75	111	24	58	15.1
D5	8.9	0.08	23.11	7.70	15.40	2.11	6	32.1	23.8	250	414	246	334	232	260	145	75	115	25	61	13.7
E1	9.2	0.048	14.55	4.85	9.70	2.31	6	24.3	18.0	211	429	196	200	251	236	89	54	82	21	44	10.2
E2	9.1	0.049	14.59	4.86	9.73	2.22	6	25.2	18.7	232	428	231	240	250	256	111	67	92	22	46	14.0
E3	9.0	0.049	14.03	4.68	9.35	1.85	6	23.7	17.6	258	428	256	285	249	272	110	72	94	22	49	15.0
E4	9.1	0.049	14.17	4.72	9.45	1.84	6	23.3	17.2	277	429	275	340	254	293	110	74	95	22	50	15.9

^aThe stoichiometric oxygen excess.

^b $F_{h1} / F_{h2} \approx 1.3-1.4$.

^c $t_{15} = t_{16} = t_{17}$.

^d $t_{21} = t_{24}$.

^eThe mass flow of cooling water $F_{cw} = 90 \text{ kg/h}$ (constant).

^fURT: The URT is the time that reagents stay inside the reactor under supercritical temperature, and it can be calculated using the piecewise average flow rate and density of the mixture [27].

Besides, the pressure of experimental system $p = 23 \text{ MPa}$. The temperatures ($t_1, t_2, t_3, t_4, t_7, t_8, t_9, t_{12}, t_{14}, t_{22}$) not listed in the table are at room temperature.

$$Q_{h2} = F_{tw1}(h_{10} - h_9) \quad (8)$$

$$Q_{h3} = F_{cw}(h_{23} - h_{22}) \quad (9)$$

4. Results and discussion

4.1. The effect of operating parameters on energy consumption

In this section, the effect of operating parameters including feed concentration, feed temperature, feed flow, transpiration intensity, and the temperature of the upper branch of transpiring water, on ECPT was analyzed. The operating conditions and some results are shown in Table 1. t_1 – t_{24} are the stream temperatures shown in Fig. 1.

4.1.1. Feed concentration

The operating conditions and results of the effect of feed concentration on ECPT are listed in Table 1 (experiments: A1–A4) with other operating parameters. Higher feed concentrations which correspond to

higher reaction temperatures and fast reaction rate are favorable to the degradation of feed [30,31], thus higher TOC removal efficiencies are present at higher feed concentrations (Fig. 3(c)). The heat released by SCWO of feed increases linearly with feed concentration as shown in Eqs. (4–6). Q_r increased from 1.29 to 5.16 kW when feed concentration was increased from 2 to 8 wt.% (Fig. 3(a)). Therefore, higher outlet temperatures (t_{15}) of the reactor are present at higher feed concentrations.

Q_{h1} , Q_{h2} , and Q_{h3} increase when feed concentration is increased; hence, Q_{e1} and Q_{e2} (Fig. 3(a)) decrease. When feed concentration is increased from 2 to 8 wt.%, the total energy recovery of heat exchangers continuously increases from 10.89 to 12.83 kW (Fig. 3(b)), and the total energy consumption of the three electric heaters decreases from 15.93 to 14.87 kW. The total energy consumption of the system decreases and the total TOC removal increases, when feed concentration is increased. Therefore, ECPT is continuously reduced from 180.16 to 56.62 kW/kg (Fig. 3(c)).

Although, lower ECPT is present at high feed concentrations, high reaction temperatures appears at high feed concentrations, which may lead to overheat-

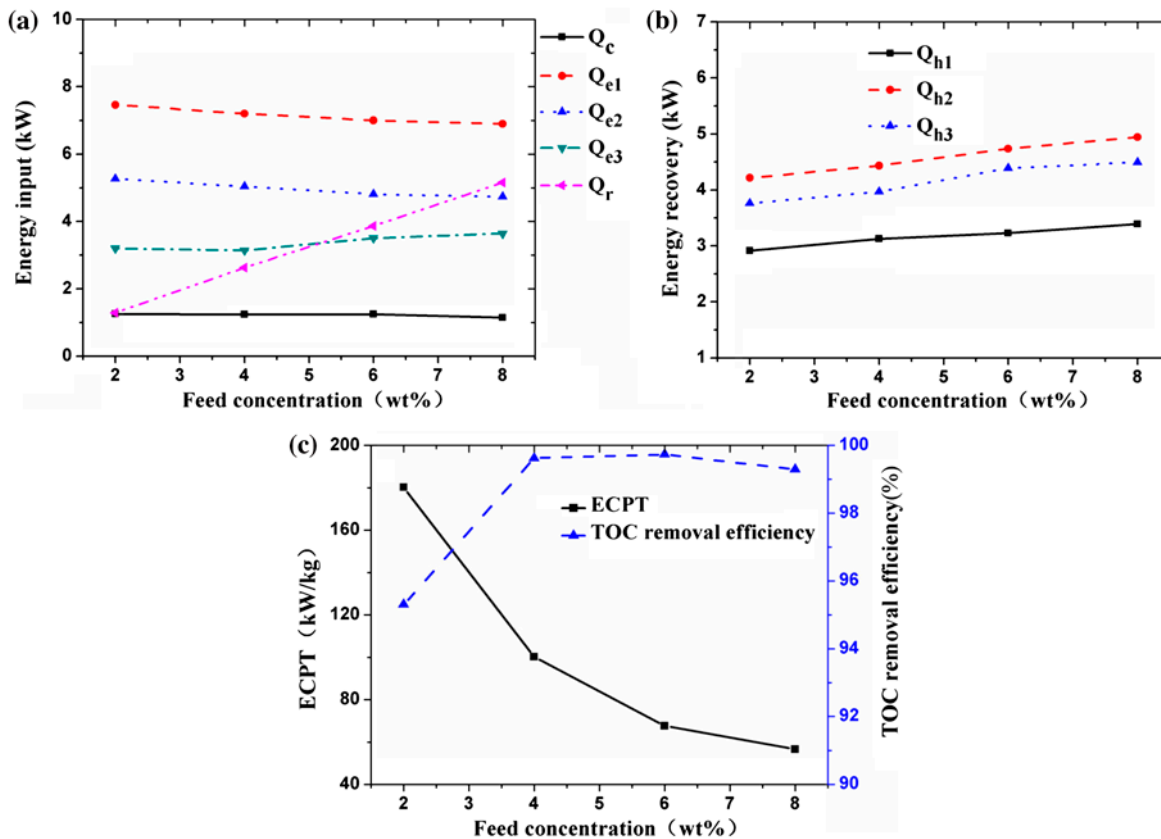


Fig. 3. The effect of feed concentration on ECPT: (a) energy input, (b) energy recovery, (c) ECPT and TOC removal.

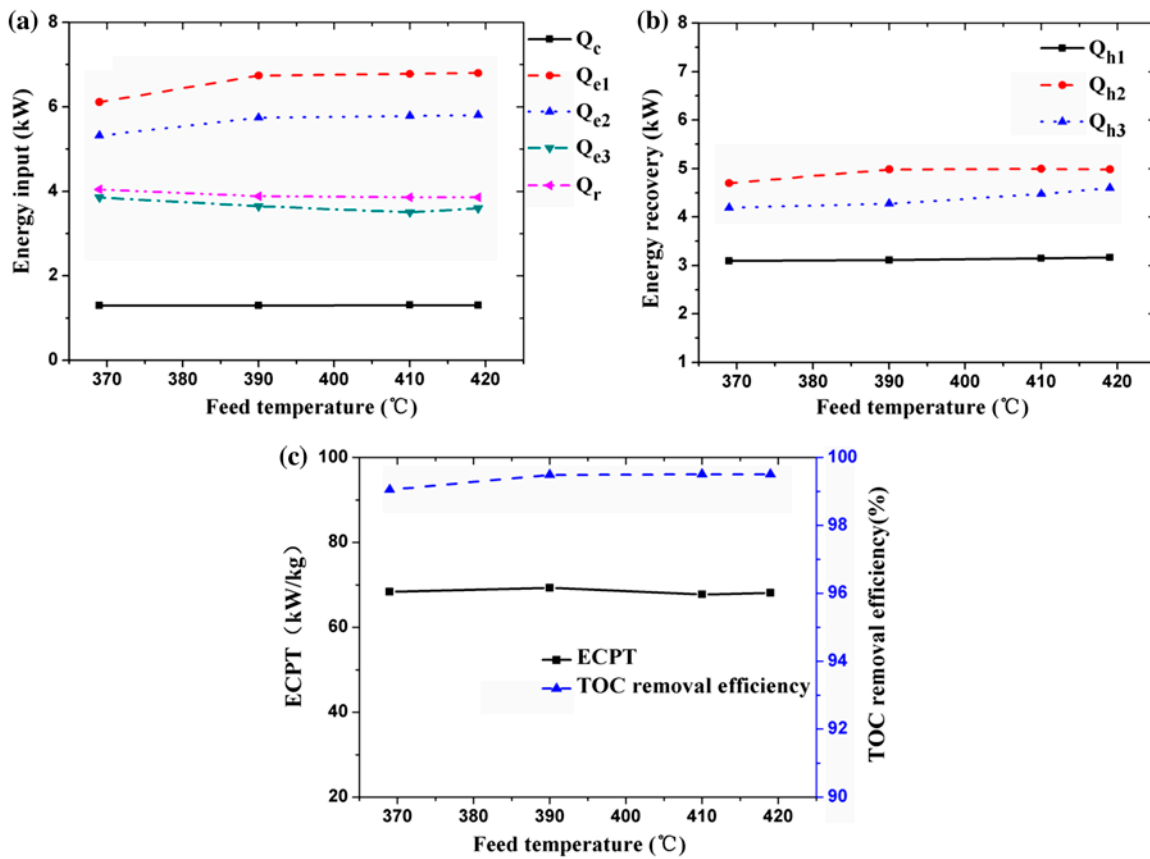


Fig. 4. The effect of feed temperature on ECPT: (a) energy input, (b) energy recovery, (c) ECPT and TOC removal.

ing the reactor [23,32]. A material with higher temperature-resistant performance is required for the reactor, which increases the investment cost of the system. Moreover, SCWO may be more expensive than other wastewater treatment at higher feed concentrations, such as incineration [12,26].

4.1.2. Feed temperature

The operating conditions and results of the effect of feed temperature on ECPT are listed in Table 1 (experiments B1–B4). Feed temperature is a key parameter for the initiation of an SCWO reaction [30,33]. The SCWO reaction did not initiate until the feed temperature was raised to 369°C at corresponding operating condition. Q_{e1} increases when feed temperature is increased and large increase are present from 369 to 400°C (Fig. 4(a)). Feed temperature has little influence on energy input and energy recovery when feed temperature is above 400°C (Fig. 4(a) and (b)). This can be explained by the specific enthalpy of water with a sharp gradient near the critical point as shown in Fig. 5. The enthalpy growth rate from 0 to 360°C is 4.75 kJ/(kg°C), but rises to 24.45 kJ/(kg°C)

from 360 to 400°C, and declines to about 4.5 kJ/(kg°C) when temperature is above 400°C; therefore, more energy is needed when water is preheated from subcritical temperature to supercritical temperature. Results show the minor influence of feed temperature

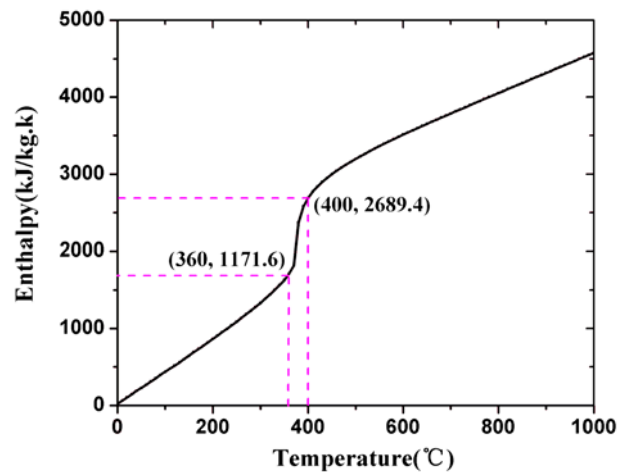


Fig. 5. The variation of the specific enthalpy of water with temperature at $p = 23$ MPa.

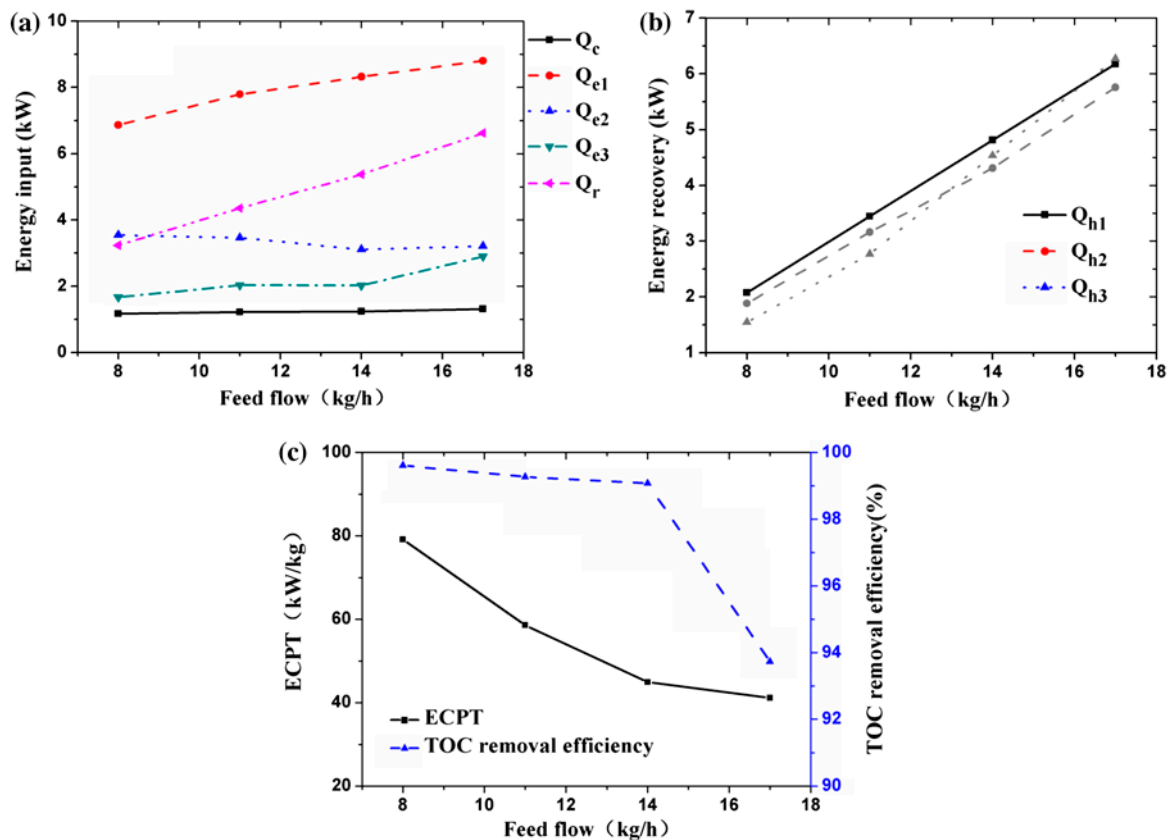


Fig. 6. The effect of feed flow rate on ECPT: (a) energy input, (b) energy recovery, (c) ECPT and TOC removal.

on TOC removal efficiency and ECPT (Fig. 4(c)). Feed temperature is usually chosen to be as low as possible on the premise of the initiation of SCWO reaction.

4.1.3. Feed flow rate

The operating conditions and results of the effect of feed flow rate on ECPT are listed in Table 1 (experiments C1–C4). When feed flow rate is increased, the flow rates of oxygen and transpiring water increase in proportion; hence, Q_c , Q_r , and Q_{e3} increase (Fig. 6(a)). The outlet flow rate ($F_{h1} + F_{h2}$) and temperature (t_{15}) of the reactor significantly increase when feed flow is increased. The ratio of F_{h1} and F_{h2} is normally kept at 1.3–1.4, therefore, F_{h1} and F_{h2} will also increase with the increase of feed flow rate. For h1 and h2, the heat transfer coefficient of the inner and outer surface of the center tube will greatly increase because of the increase of velocity of streams in both center tube and outer tube [15,34]. Total energy recovery of heat exchangers increases from 5.51 kW at 8 kg/h to 18.20 kW at 17 kg/h (Fig. 6(b)). Q_{e2} decreases but Q_{e1} increases because more energy is required to preheat

feed to a supercritical temperature as illustrated in Fig. 5. The increase of feed flow benefits the decrease of ECPT, which declines from 79.11 kW/kg at 8 kg/h to 41.15 kW/kg at 17 kg/h (Fig. 6(c)).

The feed flow rate represents the throughput of the reactor, thus higher feed flows are proposed. TOC removal efficiency is reduced from 99.61% at 14 kg/h to 93.73% at 17 kg/h (Fig. 6(c)) for the decline of useful residence time (URT) [27]. Therefore, high feed flow rates oppose the degradation of feed because of the significantly declines of useful resident time [34]. Feed flow rate should thus be increased as much as possible based on high TOC removal efficiency.

4.1.4. Transpiration intensity

The operating conditions and results of the effect of transpiration intensity on energy consumption are listed in Table 1 (experiments D1–D5). For a fixed feed flow rate, the flow rate of transpiring water will increase when the transpiration intensity increases. Although, the outlet flow rates of the reactor ($F_{h1} + F_{h2}$)

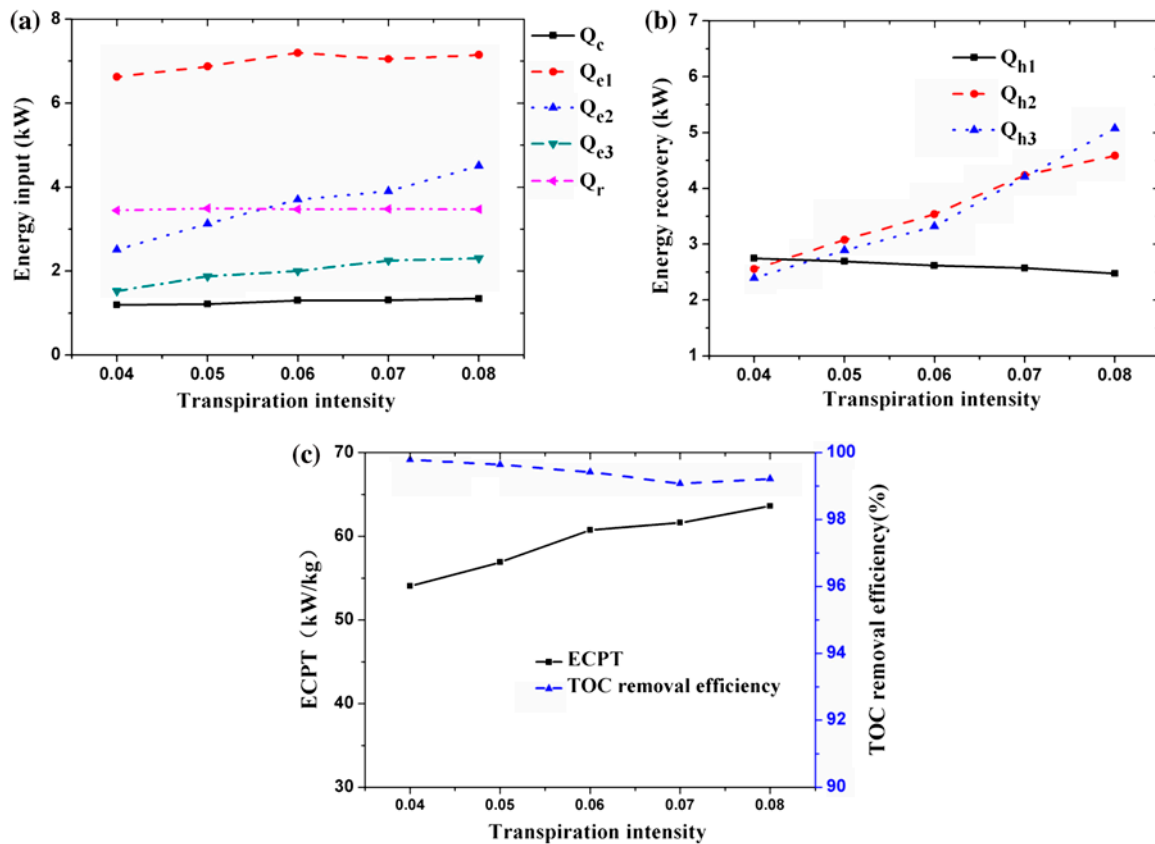


Fig. 7. The effect of transpiration intensity on ECPT: (a) energy input, (b) energy recovery, (c) ECPT and TOC removal.

are higher, the outlet temperatures (t_{15}) are much lower at higher transpiration intensities because of the cooling of the transpiring water. Although the TOC removal efficiency can exceed 99% at transpiration intensity of 0.04–0.08 (Fig. 7(c)), higher transpiration intensities will decrease the energy grades of the reactor effluent.

Although both F_{h1} and F_{h2} increased, energy recovery for h1 is decreased due to lower inlet temperatures of hot stream at higher transpiration intensities (Fig. 7(b)). Energy recovery for h2 and h3 increases rapidly because of the velocity increase of hot stream. Although the total energy recovery of heat exchangers increases, its increment is usually lower than the total energy consumption of three electric heaters and air compressor (Fig. 7(a)). ECPT increased from 54.03 kW/kg at $R=0.04$ –63.60 kW/kg at $R=0.08$ (Fig. 7(c)). On the other hand, higher transpiring intensity can provide more cooling water and higher velocities on the inner surface of the porous wall which are favorable to anticorrosion and salt plugging performance of the reactor [23,28,29]. Thus, the proper transpiration intensity should be a compromise

between ECPT and the anticorrosion and salt plugging performance of the reactor.

4.1.5. The temperature of the upper branch of transpiring water

The operating conditions and results of the effect of $tw1$ on ECPT are listed in Table 1 (experiments E1–E4). The outlet temperatures are higher at higher $tw1$ temperatures. Energy recovery of three heat exchangers increases when $tw1$ temperature increases, resulting in Q_{e1} declining but Q_{e2} increasing (Fig. 8(a) and (b)). ECPT increases from 56.87 kW at 195°C to 70.53 kW at 340°C (Fig. 8(c)).

The temperature of $tw1$ has a direct effect on the reaction zone [28,35], and TOC removal efficiency is compromised at lower temperatures. The experimental results show more than 99% TOC removal efficiency which is achieved at the temperature above 285°C. Moreover, the temperature of $tw1$ is the most important factor to form the “subcritical water film” that protects the reactor [28,35,36]. A comprehensive consideration of the formation of “subcritical water

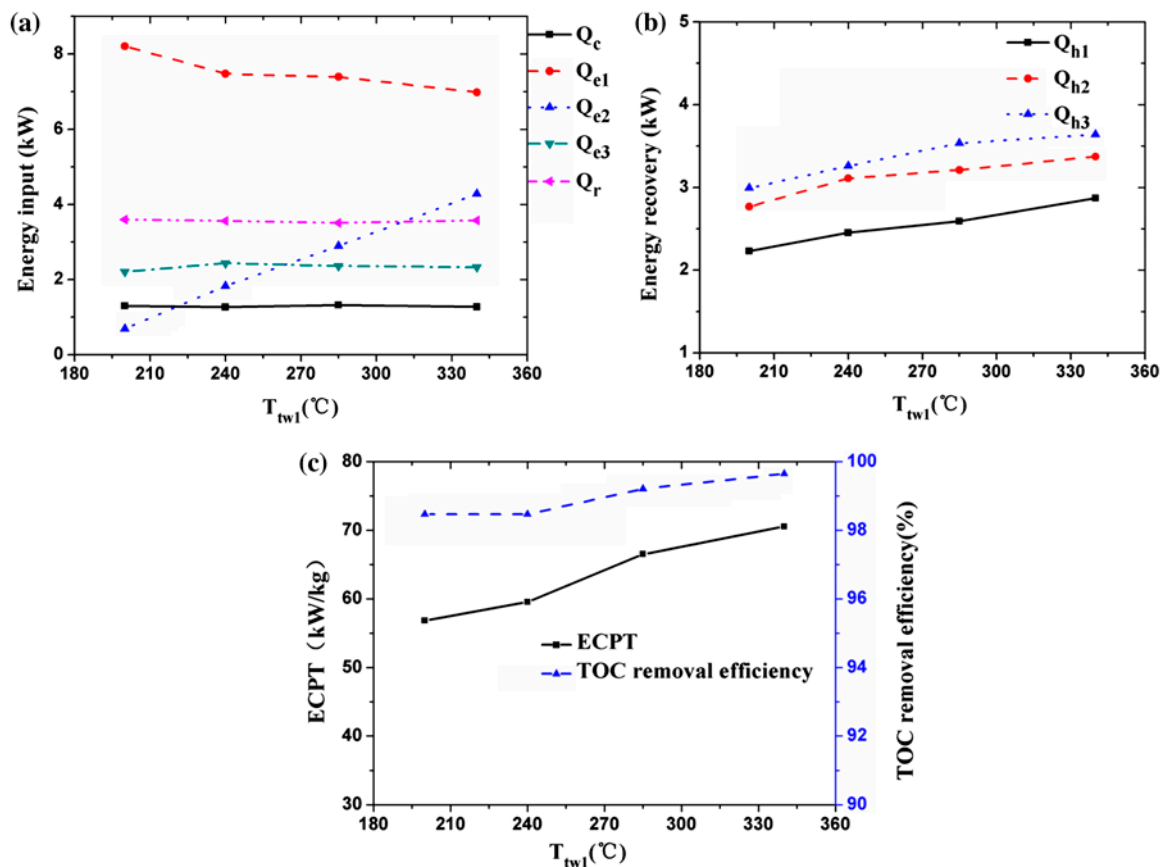


Fig. 8. The effect of the temperature of tw_1 on ECPT: (a) energy input, (b) energy recovery, (c) ECPT and TOC removal.

film," TOC removal efficiency and ECPT should be conducted to select the proper temperature of tw_1 .

4.2. Hot water production

A constant mass flow of cooling water at 90 kg/h is set at all experiments to ensure the reactor effluent is cooled to approximately 80°C (maximal operating temperature of the back pressure valve). Hot water between 40 and 75°C was produced in the pilot plant as shown in Table 1. According to the standard of hot water for residents in China, the appropriate temperature of hot water is about 60–70°C, so the mass flow of cooling water can be adjusted to match the standard.

5. Conclusion

Energy self-sufficiency is usually difficult to realize in a transpiring wall SCWO system because of the lower temperatures of reactor effluent. An alternative to maximize the energy recovery in transpiring wall

SCWO pilot plant was provided. To gain the maximum energy recovery, the effluent from the reactor in the pilot plant is not only used to preheat feed and transpiring water, but also to supply hot water as well. The new process was estimated by ECPT.

Results show that the effect of feed concentration on ECPT is the most significant, and that of higher feed concentrations, results in lower ECPT. Lower ECPT is present at higher feed flow rates, but this is at the expense of the decrease of TOC removal efficiency when feed flow rate exceeds 14 kg/h. The feed temperature has minor influence on ECPT. The thermal energy grade is decreased at higher transpiration intensities, which result in higher ECPT. Lower temperatures of tw_1 are proposed to reduce ECPT and form the subcritical "water film."

The investigation of the influence of operating parameters on ECPT provided optimized operating parameters for energy saving which has never been mentioned in previous studies. The finding from the present study can also guide the improvement direction for transpiring wall SCWO systems.

Nomenclature

A	—	area m^2
b	—	inner circular of the porous wall
cw	—	cooling water
$e1$	—	electric heater 1
$e2$	—	electric heater 2
$e3$	—	electric heater 3
ECPT	—	energy consumption per unit TOC removal
F	—	mass flow rate kg/h
$h1$	—	heat exchanger 1
$h2$	—	heat exchanger 2
$h3$	—	heat exchanger 3
ΔH_f^0	—	standard enthalpy of formation kJ/mol
M	—	molar mass of CH_4O kg/mol
q_r	—	specific reaction heat kW/kg
Q	—	heat electric energy kW
R	—	transpiration intensity
t	—	temperature $^{\circ}C$
tw	—	transpiring water
$tw1$	—	the upper branch of transpiring water
$tw2$	—	the middle branch of transpiring water
$tw3$	—	the lower branch of transpiring water
TOC	—	total organic carbon
X	—	TOC removal efficiency

Subscripts

b	—	the inner circular of the porous wall
ox	—	oxygen
w	—	organic waste water
r	—	reaction, reactor

Greek symbols

γ	—	stoichiometric oxygen excess
ω	—	feed concentration $wt.\%$

Acknowledgments

This work is supported by the National High Technology Research and Development Program (863 Program) (No. 2007AA05Z235), Research Programs of Resource-saving Society Science and Technology Special Project Support System of Shandong Province (No. 2006JY28), and Graduate Independent Innovation Foundation of Shandong University, GIIFSDU (No. yzc10124), China.

References

- [1] F. Donatini, G. Gigliucci, J. Riccardi, M. Schiavetti, R. Gabbrielli, S. Briola, Supercritical water oxidation of coal in power plants with low CO_2 emissions, *Energy* 34 (2009) 2144–2150.
- [2] N. Akiya, P.E. Savage, Roles of water for chemical reactions in high-temperature water, *Chem. Rev.* 102 (2002) 2725–2750.
- [3] P.E. Savage, Organic chemical reactions in supercritical water, *Chem. Rev.* 99 (1999) 603–621.
- [4] A. Kruse, E. Dinjus, Hot compressed water as reaction medium and reactant: Properties and synthesis reactions, *J. Supercrit. Fluids* 39 (2007) 362–380.
- [5] O.O. Sogut, E.K. Yildirim, M. Akgun, The treatment of wastewaters by supercritical water oxidation, *Desalin. Water Treat.* 26 (2011) 131–138.
- [6] Jiaming Zhang, Chunyuan Ma, Fengming Zhang, Supercritical water oxidation of N-phenylglycinonitrile wastewater, *Desalin. Water Treat.* 2013, accepted.
- [7] A. Kruse, E. Dinjus, Hot compressed water as reaction medium and reactant: 2. Degradation reactions, *J. Supercrit. Fluids* 41 (2007) 361–379.
- [8] J.W. Griffith, D.H. Raymond, The first commercial supercritical water oxidation sludge processing plant, *Waste Manage.* 22 (2002) 453–459.
- [9] B. Veriansyah, J.D. Kim, Supercritical water oxidation for the destruction of toxic organic wastewaters: A review, *J. Environ. Sci.* 19 (2007) 513–522.
- [10] P.A. Marrone, S.D. Cantwell, D.W. Dalton, SCWO System Designs for Waste Treatment: Application to Chemical Weapons Destruction, *Ind. Eng. Chem. Res.* 44 (2005) 9030–9039.
- [11] H. Schmieder, J. Abeln, Supercritical water oxidation: State of the art, *Chem. Eng. Technol.* 22 (1999) 903–908.
- [12] P. Kritzer, E. Dinjus, An assessment of supercritical water oxidation (SCWO) existing problems, possible solutions and new reactor concepts, *Chem. Eng. J.* 83 (2001) 207–214.
- [13] M.D. Bermejo, M.J. Cocero, Supercritical water oxidation: A technical review, *AIChE J.* 52 (2006) 3933–3951.
- [14] P.A. Marrone, M. Hodes, K.A. Smith, J.W. Tester, Salt precipitation and scale control in supercritical water oxidation—part B: Commercial/full-scale applications, *J. Supercrit. Fluids* 29 (2004) 289–312.
- [15] D. Kodra, V. Balakotaiah, Autothermal oxidation of dilute aqueous wastes under supercritical conditions, *Ind. Eng. Chem. Res.* 33 (1994) 575–580.
- [16] E.D. Lavric, H. Weyten, J.D. Ruyck, V. Plesu, V. Lavric, Delocalized organic pollutant destruction through a self-sustaining supercritical water oxidation process, *Energy Convers. Manage.* 46 (2005) 1345–1364.
- [17] M.J. Cocero, E. Alonso, M.T. Sanz, F. Fdz-Polanco, Supercritical water oxidation process under energetically self-sufficient operation, *J. Supercrit. Fluids* 24 (2002) 37–46.
- [18] M.D. Bermejo, M.J. Cocero, F. Fernández-Polanco, A process for generating power from the oxidation of coal in supercritical water, *Fuel* 83 (2004) 195–204.
- [19] F. Marias, F. Mancini, F. Cansell, J. Mercadier, Energy recovery in supercritical water oxidation process, *Environ. Eng. Sci.* 25 (2008) 123–130.
- [20] E.D. Lavric, H. Weyten, J. De Ruyck, V. Plesu, V. Lavric, Supercritical water oxidation improvements through chemical reactors energy integration, *Appl. Therm. Eng.* 26 (2006) 1385–1392.
- [21] J. Abeln, M. Kluth, M. Bottcher, W. Sengpiel, Supercritical water oxidation (SCWO) Using a transpiring wall reactor: CFD simulations and experimental results of ethanol oxidation, *Environ. Eng. Sci.* 21 (2004) 93–99.
- [22] P.J. Crooker, K.S. Ahluwalia, Z. Fan, J. Prince, Operating results from supercritical water oxidation plants, *Ind. Eng. Chem. Res.* 39 (2000) 4865–4870.
- [23] K. Pr'kopsky', B. Wellig, P. Rudolf von Rohr, SCWO of salt containing artificial wastewater using a transpiring wall reactor: Experimental results, *J. Supercrit. Fluids* 40 (2007) 246–257.

- [24] M.D. Bermejo, Á. Martín, J.P.S. Queiroz, I. Bielsa, R. Vicente, M.J. Cocero, Computational fluid dynamics simulation of a transpiring wall reactor for supercritical water oxidation, *Chem. Eng. J.* 158 (2010) 431–440.
- [25] F. Jimenez-Espadafor, J.R. Portela, V. Vadillo, J. Sánchez-Oneto, J.A. Becerra Villanueva, M. Torres García, E.J. Martínez de la Ossa, Supercritical water oxidation of oily wastes at pilot plant: simulation for energy recovery, *Ind. Eng. Chem. Res.* 50 (2011) 775–784.
- [26] S.N.V.K. Aki, M.A. Abraham, An economic evaluation of catalytic supercritical water oxidation: Comparison with alternative waste treatment technologies, *Environ. Prog.* 17 (1998) 246–255.
- [27] Fengming Zhang, Shouyan Chen, Chunyuan Xu, Guifang Chen, Jiaming Zhang, Chunyuan Ma, Experimental study on the effects of operating parameters on the performance of a transpiring-wall supercritical water oxidation reactor, *Desalination*, 294 (2012) 60–66.
- [28] B. Wellig, K. Lieball, P. Rudolf Von Rohr, Operating characteristics of a transpiring-wall SCWO reactor with a hydrothermal flame as internal heat source, *J. Supercrit. Fluids* 34 (2005) 35–50.
- [29] M.D. Bermejo, F. Fdez-Polanco, M.J. Cocero, Experimental study of the operational parameters of a transpiring wall reactor for supercritical water oxidation, *J. Supercrit. Fluids* 39 (2006) 70–79.
- [30] B. Wellig, M. Weber, K. Lieball, K. Pr'kopsky, P. Rudolf von Rohr, Hydrothermal methanol diffusion flame as internal heat source in a SCWO reactor, *J. Supercrit. Fluids* 49 (2009) 59–70.
- [31] F. Vogel, J.L.D. Blanchard, P.A. Marrone, F.S. Rice, P.A. Webley, W.A. Peters, K.A. Smith, J.W. Tester, Critical review of kinetic data for the oxidation of methanol in supercritical water, *J. Supercrit. Fluids* 34 (2005) 249–286.
- [32] M.D. Bermejo, F. Fdez-Polanco, M.J. Cocero, Effect of the transpiring wall on the behavior of a supercritical water oxidation reactor: Modeling and experimental results, *Ind. Eng. Chem. Res.* 45 (2006) 3438–3446.
- [33] C. Narayanan, C. Frouzakis, K. Boulouchos, K. Pr'kopsky, B. Wellig, P. Rudolf von Rohrb, Numerical modelling of a supercritical water oxidation reactor containing a hydrothermal flame, *J. Supercrit. Fluids* 46 (2008) 149–155.
- [34] V. Kumar, B. Faizee, M. Mridha, K.D.P. Nigam, Numerical studies of a tube-in-tube helically coiled heat exchanger, *Chem. Eng. Process.* 47 (2008) 2287–2295.
- [35] M.D. Bermejo, M.J. Cocero, Destruction of an industrial wastewater by supercritical water oxidation in a transpiring wall reactor, *J. Hazard. Mater.* 137 (2006) 965–971.
- [36] K. Pr'kopsky, B. Wellig, P. Rudolf von Rohr, SCWO of salt containing artificial wastewater using a transpiring-wall reactor: Experimental results, *J. Supercrit. Fluids* 40 (2007) 246–257.